Bond selective dissociation of methane (CH_3D) on the steps and terraces of Pt(211)

Ana Gutiérrez-González, F. Fleming Crim, and Rainer D. Beck

Citation: The Journal of Chemical Physics **149**, 074701 (2018); doi: 10.1063/1.5041349
View online: https://doi.org/10.1063/1.5041349
View Table of Contents: http://aip.scitation.org/toc/jcp/149/7
Published by the American Institute of Physics

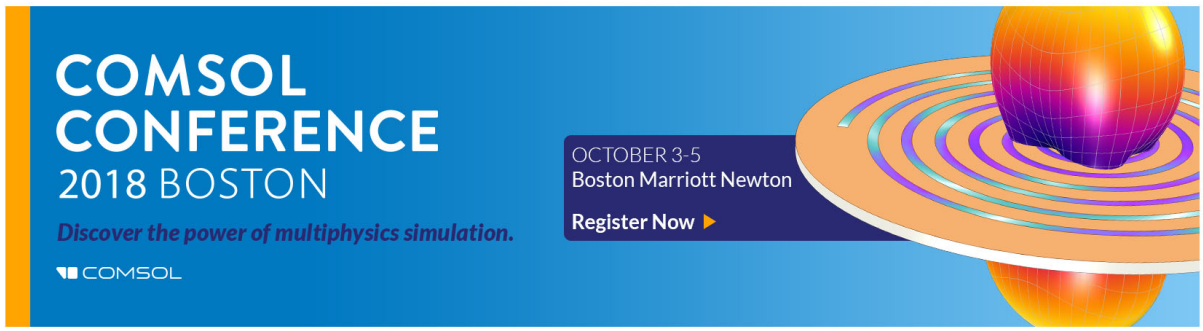

Bond selective dissociation of methane (CH_3D) on the steps and terraces of Pt(211)

Ana Gutiérrez-González,[1] F. Fleming Crim,[2] and Rainer D. Beck[1,a)]
[1]*Laboratoire de Chimie Physique Moléculaire, Ecole Polytechnique Fédérale de Lausanne, 1015 Lausanne, Switzerland*
[2]*Department of Chemistry, University of Wisconsin, Madison, Wisconsin 5370, USA*

(Received 24 May 2018; accepted 6 July 2018; published online 16 August 2018)

The dissociative chemisorption of singly deuterated methane (CH_3D) has been studied on the steps and terraces of a Pt(211) surface by quantum state resolved molecular beam methods. At incident translational energy (E_t) below 50 kJ/mol, CH_3D dissociates only on the more reactive steps of Pt(211), where both C–H and C–D cleavage products CH_2D(ads) and CH_3(ads) can be detected by reflection absorption infrared spectroscopy. Vibrational excitation of a slow beam of CH_3D (E_t = 10 kJ/mol), prepared with one quantum of antisymmetric C–H stretch excitation by infrared laser pumping, allows for fully bond- and site-selective dissociation forming exclusively CH_2D(ads) on the step sites. At higher kinetic energies (E_t > 30 kJ/mol), bond selective dissociation by C–H bond cleavage is observed on the terrace sites for stretch excited CH_3D (ν_4) while on the steps, the C–H/C–D cleavage branching ratio approaches the statistical 3/1 limit. Finally, at E_t > 60 kJ/mol, both C–H and C–D cleavages are observed on both step and terrace sites of Pt(211). Our experiments show how careful control of incident translational and vibrational energy can be used for site and bond selective dissociation of methane on a catalytically active Pt surface. *Published by AIP Publishing.*
https://doi.org/10.1063/1.5041349

INTRODUCTION

Being able to control the branching ratio of a chemical reaction with several possible channels has been a long-standing goal in chemistry[1] both for practical reasons and due to the theoretical insight that the bond selective reaction control can offer. Different methods for achieving bond selectivity in chemical reactions using laser radiation have been proposed and demonstrated including femtosecond pulse timing,[2] phase control via interfering excitation pathways,[3] and vibrationally mediated reaction control.[4] The latter strategy has been shown to achieve bond selective chemistry in unimolecular dissociation,[5] bi-molecular reactions in the gas phase,[6–13] and for gas/surface reactions.[14–16]

The first observations of bond selectivity emerged from studies of gas-phase chemical reactions. Sinha *et al.*[6] reported vibrational bond selectivity for the bimolecular gas phase reaction of HOD molecules with H atoms. Their results, as well as experiments by Bronikowski *et al.*,[7], showed that vibrational excitation of the O–H bond in HOD leads almost exclusively to the H_2+OD product channel, while the excitation of the O–D stretch produced mainly HD+OH products. In the subsequent work, the two groups extended their studies to the reaction of methane isotopologues with Cl atoms. They reported bond selectivity for both C–H and C–D cleavage channels for CH_3D[8–10] and CH_2D_2[11,12] as well as an enhanced cleavage of the C–H bond for CHD_3.[12,13]

Studies of vibrational bond selectivity were subsequently extended to gas-surface reactions for methane chemisorption on nickel and platinum surfaces. The first evidence for bond selectivity in gas-surface reactions was reported by Killelea and co-workers.[14] They demonstrated bond selective dissociation of CHD_3 on Ni(111) using recombinative desorption of adsorbed methyl products with sub-surface H-atoms. Vibrational excitation with one quantum of ν_1, the unique C–H stretch in CHD_3, enhanced the C–H cleavage channel by at least 2 orders of magnitude compared to the statistical 1/3 CD_3/CHD_2 branching ratio observed without C–H stretch excitation. The Lausanne group[15,16] studied the bond selective chemisorption of all three partially deuterated methanes (CH_3D, CH_2D_2, and CHD_3) on Pt(111) using reflection absorption infrared spectroscopy (RAIRS) as the product detection method. RAIRS can be used to distinguish the different isotopologues of the methyl species on Pt(111), formed as the nascent dissociation products of the methane chemisorption. Their results show that a single quantum of C–H stretch excitation is sufficient to make the dissociation of all three methane isotopologues fully bond selective. These studies demonstrate that vibrational bond selectivity can be achieved for reactions at the gas-surface interface despite the high complexity of such systems with many possible energy relaxation channels.[17,18] The observation of strong bond selectivity clearly shows that methane chemisorption occurs via a non-statistical mechanism where the dissociating molecule at the transition state retains the memory of the initially prepared reactant state. Therefore, statistical rate theories cannot correctly describe the reaction at a microscopic level, and new

a)Electronic mail: rainer.beck@epfl.ch

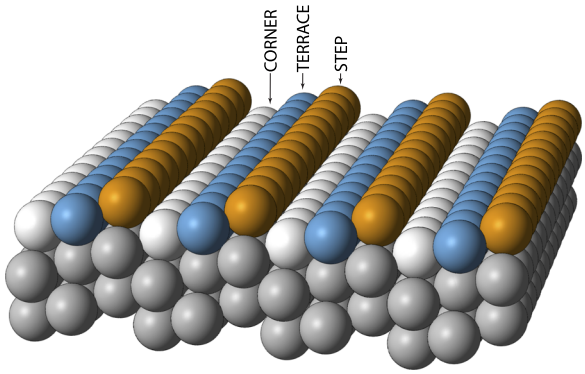

FIG. 1. Model of the Pt(211) surface with three different surface sites which are labeled as step (orange), terrace (blue), and corner site (gray).

quasi-classical and quantum theories are needed to correctly describe the reaction dynamics for this and other gas-surface systems.[16,19–21]

Here, we report the first combined study of bond- and surface-site selective dissociation of methane chemisorption. Until now, bond selectivity studies on gas-surface reactions have been done only on flat Ni(111) and Pt(111) surfaces. Molecular beam studies on more complex surfaces that resemble more closely the catalysts used in industry are still rare.[22,23] The Pt(211) surface used in this work consists of three-atom-wide terraces with the (111) structure and one-atom-high steps with (100) character. Therefore, three different surface sites (labeled as step, terrace, and corner sites in Fig. 1) are exposed to the molecular beam. In a recent publication, we have demonstrated the ability of RAIRS to distinguish between CH_3 adsorbed on the step and terrace atoms of Pt(211)[24] and measure site specific sticking coefficients for CH_4. Here, we combine this ability with quantum state-specific preparation of the incident CH_3D to investigate the degree of bond selectivity as a function of translational energy on the step and terrace sites of the Pt(211) surface.

EXPERIMENTAL METHODS

Our molecular beam-surface science apparatus combines state specific reactant preparation by infrared laser pumping using Rapid Adiabatic Passage (RAP)[25] with product detection by Reflection-Absorption-Infrared-Spectroscopy (RAIRS). Details of the design and operation of this apparatus have been described previously.[26] Briefly, a continuous molecular beam was generated from a supersonic expansion through a temperature controlled stainless steel nozzle (50 μm orifice diameter) followed by a 2 mm diameter skimmer. Before the supersonic expansion, the methane/helium gas mixtures were passed through an oxygen/moisture trap (Supelpure-O, Supelco) in order to remove any trace of O_2 and H_2O from the methane/He gas mixtures.

The translational energy of the molecular beam was controlled by seeding CH_3D in either He or Ne and by variation of the nozzle temperature (T_N). Seeding 3% CH_3D in He resulted in translational energies between 25 and 66 kJ/mol for nozzle temperatures in the range of 300-800 K. For lower translational energies, a 3% CH_3D seeded in Ne mixture was used, resulting in a translational energy of 10 kJ/mol for T_N = 500 K. The speed distribution of the molecular beam was measured by a time-of-flight method using a chopper wheel in combination with the on-axis quadrupole mass spectrometer.[27]

The molecular beam entered the ultrahigh vacuum (UHV) chamber (base pressure 5×10^{-11} mbars), where it collided at normal incidence with the circular Pt(211) surface sample (Surface Preparation Labs, Leiden) of 12 mm diameter mounted on a liquid nitrogen cryostat using 0.4 mm diameter tungsten wires.[28] The surface temperature (T_s) was controlled in the range between 90 and 1100 K using nitrogen cooling and by passing a DC current through the tungsten wires. For the deposition of vibrationally excited methane (designated laser-on), we used a continuous wave, single-mode, infrared optical parametric oscillator (cw-OPO, Aculight) to prepare 5%-34% of the surface incident CH_3D, depending on nozzle temperature and molecular beam speed, in the antisymmetric C–H stretch normal mode ν_4 and the rotational state J = 2, K = 2. The OPO idler frequency was stabilized to the $v = 0 \rightarrow \nu_4$ $R_1(1)$ transition of CH_3D by locking to a Doppler-free Lamb-dip detected in a room temperature static gas cell filled with 20 μbars of CH_3D. To maximize the excited fraction, we focused the infrared laser beam by a cylindrical CaF_2 lens into the molecular beam to achieve RAP.[25] The vibrationally excited fraction of CH_3D in the molecular beam was measured by a room temperature pyroelectric detector that could be inserted into the molecular beam before the deposition experiments.

The nascent products of CH_3D dissociation on the Pt(211) surface were detected by the RAIRS technique using an evacuated Fourier transform infrared (FTIR) spectrometer (Vertex V70). The infrared radiation, emitted from the globar source of the FTIR, was incident at 80° from the surface normal on the Pt(211) single crystal, and the reflected light was detected using an external InSb infrared detector. RAIRS detection does not interfere with the chemisorption reaction and can therefore be used to monitor the buildup of surface adsorbates during the molecular beam deposition. A RAIR absorption spectrum is obtained as the ratio of a sample spectrum recorded with the adsorbate covered surface and a background spectrum recorded with the bare surface. In this study, all spectra were recorded with 4 cm^{-1} resolution at a surface temperature of 150 K. The background spectra are an average of 8192 scans taken during 20 min acquisition time. Once the background spectrum was recorded, the surface was flashed to 1000 K to desorb possible contaminants adsorbed on the surface during the background measurement time. The surface was then cooled back to T_s = 150 K, and the molecular beam deposition started while the chemisorption product uptake was monitored by taking sample spectra averaged over 512 scans. Once the saturation coverage of methyl species was achieved, a final sample spectrum was recorded by averaging 8192 scans to achieve a high signal-to-noise ratio. Surface cleaning between measurements was done by exposing the Pt(211) crystal to 5×10^{-8} mbars of O_2 at a surface temperature of 700 K for 5 min followed by annealing at T_s = 1100 K for 2 min. At the end of each day, cleaning by Ar^+ sputtering and annealing was used. The surface cleanliness was verified using Auger Electron Spectroscopy (AES), to check that detectable (<1%

Monolayer) trace of carbon or oxygen was on the surface. Moreover, no traces of H_2O or OH groups were detected on the surface by RAIRS after the methane depositions.

RESULTS AND DISCUSSION

Figure 2(a) shows a RAIR spectrum of the nascent chemisorption products of CH_3D on Pt(211) recorded following a methane deposition to saturation without laser excitation at T_s = 150 K. The incident translational energy (E_t) of CH_3D was 66 kJ/mol obtained with a 3% CH_3D in the He mixture for a nozzle temperature of T_N = 800 K. Due to inefficiency of vibrational cooling in the supersonic expansion,[29] the incident CH_3D contains 9.3 kJ/mol of thermal vibrational energy as calculated from the vibrational partition function, yielding a total energy of the incident CH_3D of 75.3 kJ/mol. Previous RAIRS measurements[15] showed that CH_3D dissociates on the terrace sites of Pt(111), both by C–H and C–D bond cleavage resulting in the nascent products CH_2D(ads) or CH_3(ads) [see Fig. 2(b)] which can readily be distinguished by RAIRS. The Pt(211) surface comprises three different types of surface atoms which we designate as step, terrace, and corner sites (see Fig. 1). For CH_4 dissociation on Pt(211), we reported that the dissociation product CH_3(ads) can be detected with surface site selectivity on both the step and terrace sites and that no dissociation products were detected on the corner sites consistent with a much higher dissociation barrier on this site, calculated by Density Functional Theory (DFT) as 183 kJ/mol.[24]

With this information, we assign the RAIRS absorption features for the products of CH_3D dissociation on Pt(211) by comparison with the spectra for CH_3D/Pt(111), CH_4/Pt(211), and CH_4/Pt(111) taken under similar conditions

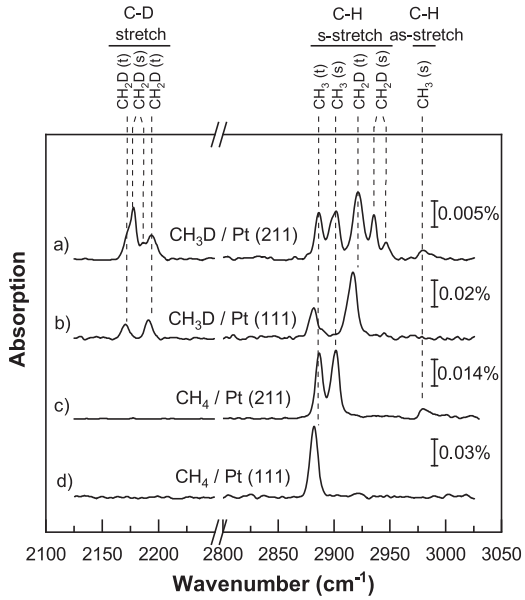

FIG. 2. (a) RAIR spectrum for the saturation coverage of chemisorbed methyl species on Pt(211) and obtained by deposition of CH_3D with E_t = 66 kJ/mol and T_s = 150 K. RAIRS features in (a) were assigned by comparison with RAIR spectra for CH_3D and CH_4 on Pt(111) and CH_4 on Pt(211) shown in (b), (c), and (d), respectively, obtained under similar conditions. Nascent methyl products adsorbed on step and terrace sites are labeled (s) and (t), respectively.

[Figs. 2(b)–2(d)]. The observed vibrational frequencies are given with their assignments in Table I.

We note that in the C–H stretch region (2850-3000 cm^{-1}), the absorption due to CH_2D(ads) on the step sites is split into a doublet separated by 11 cm^{-1}. In the C–D stretch region, both the step and the terrace peaks due to CH_2D(ads) are split and only partially resolved. These splittings are likely due to anharmonic coupling of CH_2D(ads) vibrations. We exclude orientation effects of the CH_2D(ads) on the step sites from being responsible for the observed splitting based on DFT calculations which predict the methyl groups to be freely rotating. Therefore, the precise origin of the observed splitting is currently unknown.

Figure 2(a) also shows a peak at 2979 cm^{-1} which we assign as the antisymmetric C–H stretch of CH_3(ads) on the steps sites. On the terrace sites, this peak is not observed due to the surface selection rule for RAIRS which states that only adsorbate vibrations with a transition dipole component along the surface normal[30] can be detected. For the CH_3(ads) on the terrace site, with a local symmetry of C_{3v}, there is no dipole moment component along the surface normal for the antisymmetric C–H stretch mode. However, for CH_3(ads) on the step sites, a small tilt angle of the methyl group's C_{3v} axis away from the microscopic surface normal can lead to a small dipole component along the surface normal.

Figure 2(a) shows that RAIRS detection on Pt(211) lets us distinguish between the product species CH_2D(ads) and CH_3(ads) on the step and the terrace adsorption sites. We can therefore use RAIRS to study the bond selective dissociation of CH_3D with site selectivity both on the step and the terrace sites. To probe the extent of translational and vibrational activation of CH_3D dissociation on Pt(211), we performed deposition experiments at different incident translational energies, with and without laser excitation of the C–H stretch mode ν_4. Figure 3(a) shows a series of laser-off RAIR spectra, each taken following deposition of a molecular beam of CH_3D to create a saturation coverage of methyl products for several different translational energies (E_t). In previous work,[24] we have shown that at the low surface temperature used in our experiments, diffusion of the methyl species on the Pt(211) surface does not occur. For E_t = 10-58 kJ/mol, CH_3D dissociation is detected exclusively on the step sites by either C–H or C–D cleavage. For $E_t \geq 58$ kJ/mol, dissociation of CH_3D starts to occur also on the terrace sites, signalling a lower CH_3D reactivity on the terrace than on the step sites. These results agree well with measurements and calculations for CH_4 dissociation

TABLE I. Assignments of RAIRS features observed for nascent methyl products of CH_3D dissociation on Pt(211) at T_s = 150 K. Peak frequencies are taken from the spectrum of Fig. 2(a).

Methyl	Frequency (cm^{-1}) Terraces	Steps	Mode assignment
CH_3(ads)	2886	2903	Symmetric C–H stretch
		2979	Antisymmetric C–H stretch
CH_2D(ads)	2921	2936 and 2947	Symmetric C–H stretch
	2173 and 2194	2178 and 2186	C–D stretch

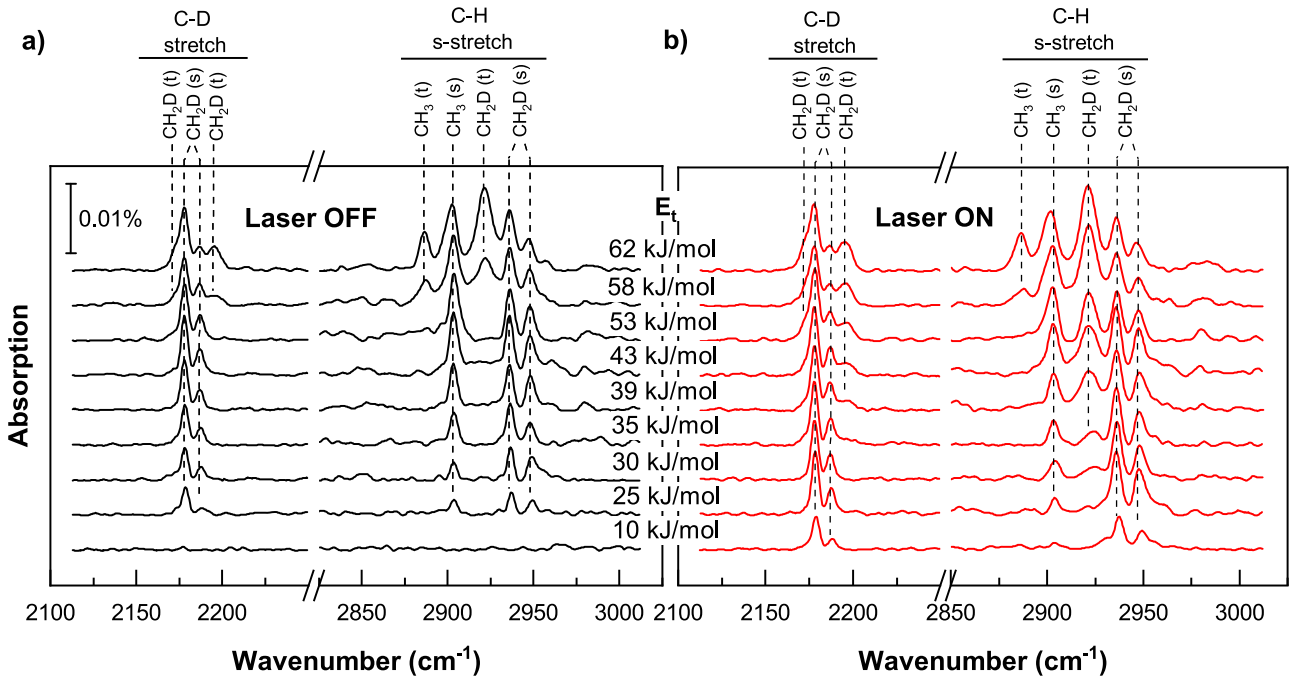

FIG. 3. RAIR spectra following dissociation of CH_3D on Pt(211) as a function of incident translational energy E_t without [laser-off, panel (a)] and with state specific ν_4 C–H stretch excitation [laser on, panel (b)].

on Pt(211) where the barrier for CH_4 dissociation on Pt(211) was found to be higher on the terraces (84 kJ/mol) than on the steps (42 kJ/mol).[24]

Figure 3(b) shows RAIR spectra obtained following laser-on depositions to saturation of CH_3D on Pt(211) at different incident energies. IR pumping prepared a fraction of the incident CH_3D with 36 kJ/mol of vibrational energy in the C–H antisymmetric stretch normal mode ν_4. Comparison of the spectra in Figs. 3(a) and 3(b) for the same translational energies shows the effect of ν_4 excitation on the dissociative chemisorption for both the step and terrace sites. At the lowest translational energy E_t = 10 kJ/mol, where no chemisorbed products were detected for the laser-off deposition, fully bond- and site-selective dissociation occurs for ν_4-excited CH_3D, dissociating only by C–H cleavage and exclusively on the step sites. For $E_t \geq 25$ kJ/mol, C–D cleavage (to produce CH_3) now starts to occur on the steps, but an enhancement of the C–H over C–D cleavage is still observable, which decreases with increasing E_t. For E_t = 39-53 kJ/mol, bond selectivity switches from the step to the terrace sites, leaving exclusively the C–H cleavage product on the terraces. The C–D cleavage product CH_3(ads) on the terraces appears only for $E_t \geq 58$ kJ/mol.

To quantify the degree of bond selectivity, we compared the product yield for C–H and C–D cleavage channels, leading to CH_2D(ads) and CH_3(ads) products, respectively, both for the step and terrace sites at saturation coverage. Here, we calibrate the relative RAIRS intensities in terms of coverage for CH_2D(ads) and CH_3(ads), assuming that the C–H/C–D cleavage branching ratio has reached the statistical 3/1 limit at the highest incident translational energy (E_t = 66 kJ/mol) for the laser-off experiments. This assumption was confirmed in previous measurements for the dissociation of CH_3D on Pt(111)[15] together with a linear dependence of the RAIR signals on methyl coverage.[26] Therefore, the calibrated RAIRS signals enable us to calculate the C–H/C–D branching ratios as a function of E_t for the laser-on experiments.

Since the efficiency of the vibrational excitation by RAP decreases with increasing molecular beam velocity,[25] we need to take into account the fraction of incident C–H stretch excited CH_3D (f_{exc}) in the calculation of the C–H/C–D branching ratio at different E_t. For a particular laser-on experiment, we detect the contribution from both the excited and non-excited molecules in the molecular beam. We remove the contribution

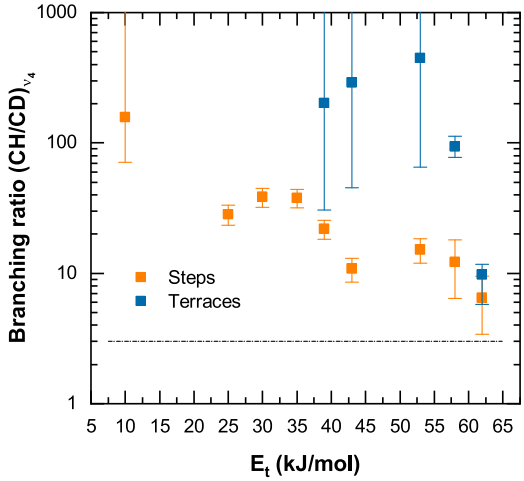

FIG. 4. CH/CD branching ratio on the steps and terraces as a function of incident kinetic energy E_t. The dashed line indicates the statistical 3/1 limit. Error bars were calculated by propagating error estimates for measured RAIRS peak areas (laser-off and laser-on) and the ν_4-excited fraction for laser-on measurements using Eq. (1).

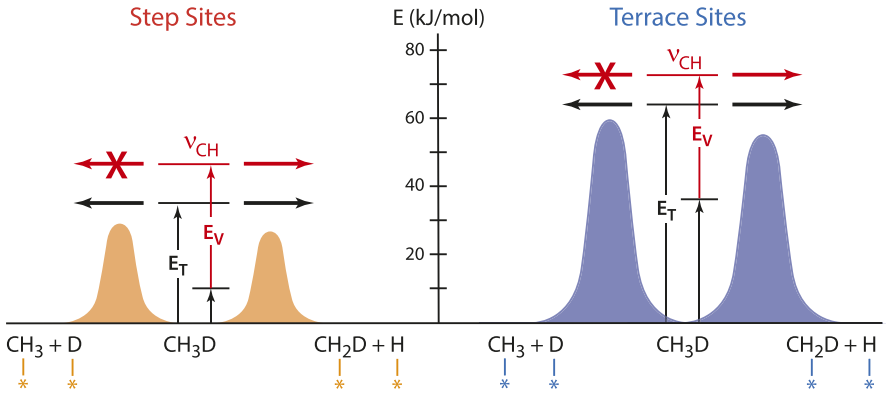

FIG. 5. Schematic of energetics and dissociation pathways for CH_3D chemisorption on the steps (left) and terraces (right) of Pt(211). For laser-off depositions, the sum of incident translational energy and thermal vibrational energy is indicated in black as E_T. Once E_T exceeds the reaction barrier, both C–H and C–D cleavage are observed with a near statistical branch ratio. State specific laser excitation of the ν_4 C–H antisymmetric stretch normal mode adds E_V = 36 kJ/mol selectively to the C–H bonds which enables bond selective C–H cleavage if the dissociation barrier cannot be overcome by E_T alone.

of the non-excited (laser-off) molecules using the data from the laser-off experiments with Eq. (1) to obtain the state resolved branching ratio $\left(\frac{CH}{CD}\right)_{\nu_4}$,

$$\left(\frac{CH}{CD}\right)_{Laser\ ON} = (1 - f_{exc})\left(\frac{CH}{CD}\right)_{Laser\ OFF} + f_{exc}\left(\frac{CH}{CD}\right)_{\nu_4}. \quad (1)$$

Figure 4 shows how the degree of bond selectivity expressed in terms of the branching ratio decreases with increasing E_t for the step and terrace sites. When full bond selectivity is observed [no CH_3(ads) is detected], we calculate only a lower limit for the C–H/C–D branching ratio based on the signal-to-noise of our RAIR spectra.

A schematic of the energetics and dissociation pathways for this reaction is shown in Fig. 5. Without state specific C–H stretch excitation of the ν_4 normal mode, only translational energy and a limited amount of thermal vibrational energy are available for dissociation of the incident CH_3D, as indicated by the black arrows. Both C–H and C–D cleavage products are detected with the nearly statistical product branching ratio once the available energy E_T exceeds the dissociation barrier height. A small preference for C–H cleavage due to the zero-point energy difference is observed. Fully bond selective dissociation is observed for incident ν_4-excited CH_3D, where 36 kJ/mol of vibrational energy are added selectively to the C–H stretch vibration, if its translational energy is well below the barrier for dissociation. This situation is shown by the red arrows in Fig. 5. Due to the different dissociation barrier heights for step and terraces sites, bond selective dissociation by C–H cleavage occurs with increasing translational energy E_t, first on the steps ($E_t \geq 10$ kJ/mol) and later for E_t = 39–53 kJ/mol on the terrace sites. Once E_t alone is sufficient to overcome the dissociation barrier, the effect of C–H excitation and the degree of bond selectivity decreases, and the branching ratio approaches the statistical 3/1 value. Figure 4 shows how the C–H/C–D branching ratio changes for dissociation of ν_4 excited CH_3D as a function of E_t between these two limiting cases where the translational energy is well below the barrier for dissociation, and full bond selectivity is observed and the case where the translational energy is above the barrier and ν_4 excitation no longer leads to bond selective dissociation. The decrease in bond-selectivity with increasing E_t observed here was predicted by quasi-classical trajectory calculations by Shen *et al.*[31] for the dissociation of partially deuterated methanes (CH_3D, CH_2D_2, and CHD_3) on Pt(111). In agreement with our interpretation given above, the authors argued that by increasing the non-selective translational energy, the influence of the bond selective vibrational excitation is diminished which alters the branching ratio toward the statistical limit.

SUMMARY

The dissociative chemisorption of CH_3D on the steps and terraces of a Pt(211) surface was studied by quantum state resolved methods using RAIRS detection of the dissociation products. The ability of this technique to distinguish between C–H and C–D cleavage products adsorbed on step- and terrace sites allowed us to study CH_3D dissociation as a function of incident translational energy E_t with surface site selectivity. We find the step sites of Pt(211) to be more reactive than the terraces. From observed changes in the RAIR spectra as a function of E_t, we estimate the difference in barrier height to be approximately 33 kJ/mol.

The C–H bond selectivity, observed for excitation of the antisymmetric C–H stretch mode ν_4, was studied for incident energies in the range of 10-62 kJ/mol. With increasing E_t, bond selectivity is first observed on the steps and then on the terrace sites. At low incident energy (E_t = 10 kJ/mol), fully bond-selective C–H cleavage occurs on the steps while dissociation on the terraces is absent, making the methane dissociation both bond- and site-selective. For E_t = 35-52 kJ/mol, both C–H and C–D cleavage occur on the steps, but full C–H bond selectivity now occurs on the terraces. Finally, for $E_t > 53$ kJ/mol, the C–H/C–D branching ratio approaches the statistical 3/1 limit on both steps and terraces. Our results indicate that when the sum of translational and thermal vibrational energy exceeds the dissociation barrier on a particular surface site, the observed bond selectivity on that site decreases. Therefore, careful tuning of the incident translational energy and control of the vibrational state of the incident CH_3D allows for both bond- and site-specific dissociation on Pt(211).

ACKNOWLEDGMENTS

R.D.B. and A.G.G. acknowledge financial support provided by the Swiss National Science Foundation (Grant Nos. P300P2-171247 and 159689/1) and the École Polytechnique Fédérale de Lausanne. F.F.C. appreciates the hospitality of EPFL during a portion of this work. We are grateful to Dr. Helen Chadwick for her help and fruitful discussions.

[1] F. F. Crim, J. Phys. Chem. **100**, 12725 (1996).
[2] N. H. Damrauer, C. Dietl, G. Krampert, S. H. Lee, K. H. Jung, and G. Gerber, Eur. Phys. J. D **20**, 71 (2002).
[3] P. Brumer and M. Saphiro, Annu. Rev. Phys. Chem. **43**, 257 (1992).
[4] F. F. Crim, Proc. Natl. Acad. Sci. U. S. A. **105**, 12654 (2008).
[5] R. L. Vander Wal, J. L. Scott, and F. F. Crim, J. Chem. Phys. **92**, 803 (1990).
[6] A. Sinha, M. C. Hsiao, and F. F. Crim, J. Chem. Phys. **92**, 6333 (1990).
[7] M. J. Bronikowski, W. R. Simpson, B. Girard, and R. N. Zare, J. Chem. Phys. **95**, 8647 (1991).
[8] S. Yoon, R. J. Holiday, and F. F. Crim, J. Phys. Chem. B **109**, 8388 (2005).
[9] S. Yoon, R. J. Holiday, E. L. Sibert, and F. F. Crim, J. Chem. Phys. **119**, 9568 (2003).
[10] R. J. Holiday, C. H. Kwon, C. J. Annesley, and F. Fleming Crim, J. Chem. Phys. **125**, 133101 (2006).
[11] H. A. Bechtel, Z. H. Kim, J. P. Camden, and R. N. Zare, J. Chem. Phys. **120**, 791 (2004).
[12] Z. H. Kim, H. A. Bechtel, and R. N. Zare, J. Am. Chem. Soc. **123**, 12714 (2001).
[13] J. P. Camden, H. A. Bechtel, D. J. Ankeny Brown, and R. N. Zare, J. Chem. Phys. **124**, 034311 (2006).
[14] D. R. Killelea, V. L. Campbell, N. S. Shuman, and A. L. Utz, Science **319**, 790 (2008).
[15] L. Chen, H. Ueta, R. Bisson, and R. D. Beck, Faraday Discuss. **157**, 285 (2012).
[16] P. M. Hundt, H. Ueta, M. E. van Reijzen, B. Jiang, H. Guo, and R. D. Beck, J. Phys. Chem. A **119**, 12442 (2015).
[17] A. M. Wodtke, D. Matsiev, and D. J. Auerbach, Prog. Surf. Sci. **83**, 167 (2008).
[18] D. R. Killelea and A. L. Utz, Phys. Chem. Chem. Phys. **15**, 20545 (2013).
[19] B. Jiang and H. Guo, J. Phys. Chem. C **117**, 16127 (2013).
[20] A. Lozano, X. J. Shen, R. Moiraghi, W. Dong, and H. F. Busnengo, Surf. Sci. **640**, 25 (2015).
[21] H. Guo and B. Jackson, J. Phys. Chem. C **119**, 14769 (2015).
[22] L. Vattuone, L. Savio, and M. Rocca, Surf. Sci. Rep. **63**, 101 (2008).
[23] J. Libuda and H. J. Freund, Surf. Sci. Rep. **57**, 157 (2005).
[24] H. Chadwick, H. Guo, A. Gutiérrez-González, J. P. Menzel, B. Jackson, and R. D. Beck, J. Chem. Phys. **148**, 014701 (2018).
[25] H. Chadwick, P. M. Hundt, M. E. van Reijzen, B. L. Yoder, and R. D. Beck, J. Chem. Phys. **140**, 034321 (2014).
[26] L. Chen, H. Ueta, R. Bisson, and R. D. Beck, Rev. Sci. Instrum. **84**, 053902 (2013).
[27] G. Scoles, *Atomic and Molecular Beam Methods* (Oxford University Press, New York, 1988).
[28] J. T. Yates, Jr., *Experimental Innovations in Surface Science* (Springer, 1999).
[29] D. K. Bronnikov, D. V. Kalinin, V. D. Rusanov, Y. G. Filimonov, Y. G. Selivanov, and J. C. Hilico, J. Quant. Spectrosc. Radiat. Transfer **60**, 1053 (1998).
[30] F. Hoffmann, Surf. Sci. Rep. **3**, 107 (1983).
[31] X. J. Shen, A. Lozano, W. Dong, H. F. Busnengo, and X. H. Yan, Phys. Rev. Lett. **112**, 046101 (2014).